

THE BERKELEY-ILLINOIS-MARYLAND-ASSOCIATION MILLIMETER ARRAY

Wm. J. Welch

Radio Astronomy Laboratory, University of California, Berkeley 94720

ABSTRACT This is a general description of the BIMA millimeter wavelength array, including some recent scientific results, the status of the expansion to a larger number of antennas, and preliminary results of attempts to correct for atmospheric "seeing". The examples of scientific results show CO images of the galaxy IC 342, emission in other spectral lines from the two regions of massive star formation SGR B2 and Orion South, and continuum emission from solar flares and the planet Mercury. There follows a brief description of the new antennas, new correlator, new receivers, and new refrigerators of the expanded array. Finally, there is a discussion of the first results from attempts to use measured fluctuations in the brightness of the atmosphere at the observing wavelength to infer the visibility phase fluctuations due to the atmosphere. Removal of the phase fluctuations using the brightness fluctuations provides a better image of a test observation of M87.

INTRODUCTION

The BIMA array consists of a number of 6m antennas arrayed as a synthesis interferometer on a T-shaped track and equipped with receivers for millimeter wavelength observations. It has stable sensitive receivers, a wide band IF, and a flexible correlation spectrometer which permits single line observations over a wide velocity range or the observation of a number of different spectral lines simultaneously. With the relatively large primary beams of its antennas, it is especially well suited to the high resolution study of extended radio sources. The array is currently being expanded from three antennas to nine.

It is evident from the large number of interesting oral and poster papers presented at this conference that the four operating millimeter arrays have been very productive during the past two to three years. All of the arrays are currently being expanded in their capabilities, so that we may expect an even greater rate of productivity in the coming years.

In the following paragraphs we briefly summarize a few highlights of current research with the BIMA array, describe the properties of the expanded array, and discuss some preliminary results of experiments designed to reduce the deleterious effects of atmospheric phase fluctuations on the construction of high resolution interferometric maps.

CURRENT RESEARCH

The scientific interests of the BIMA group and the visitors who use the array are quite varied, and the research projects span a wide range of astronomical problems. The following are a few examples.

Figure 1 shows two images of the nearby, face on Scd galaxy IC342 (Wright et al, 1992). On the left is the $^{13}\text{CO}(1-0)$ map based on observations at both BIMA and OVRO, and on the right is the $^{12}\text{CO}(1-0)$ map obtained at NRO. Resolutions are about $3''$. The comparison of the maps allows the establishment of temperatures and column densities of the CO. Peaks in the emission correspond to giant molecular clouds of diameters 20-50 pc and masses of $10^6 M_{\odot}$. The strong CO emission from the nucleus, along with both intense infrared and radio continuum, suggest a recent burst of star formation.

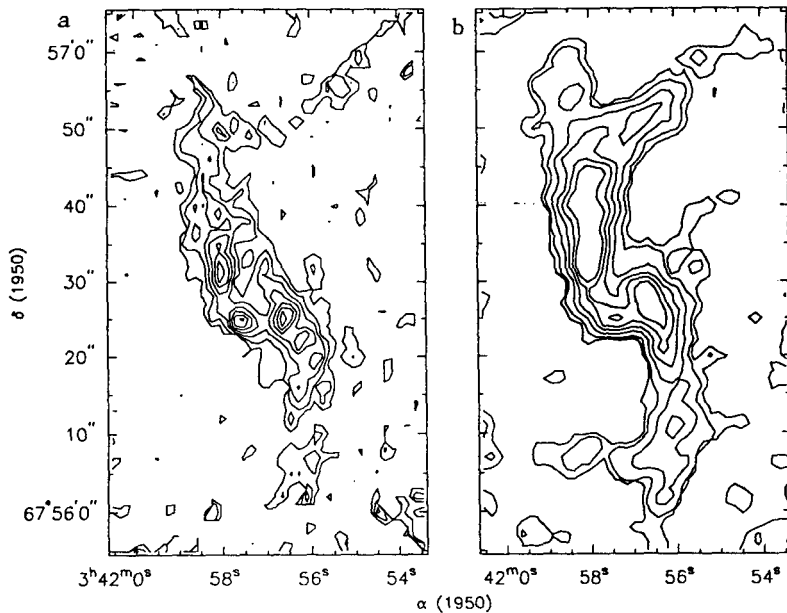


Figure 1. (a) $^{13}\text{CO}(1-0)$ map of IC342 from BIMA and OVRO. (b) $^{12}\text{CO}(1-0)$ map of IC342 from NRO.

Figure 2 shows two examples of studies of regions of high mass star formation. Figure 2a is a picture of the SGR B2 molecular cloud by Snyder et al (1992), showing the continuum emission from the middle and upper sources in gray scale. The overlaid line spectra are of $\text{CH}_3\text{CH}_2\text{CN}$ on the right and an unidentified line on the left. Although the Middle source is much brighter in the continuum than the upper source, the line features appear in only the upper source.

The multiple panels of Figure 2b show distributions of a number of molecules toward a region about two minutes south of Orion/KL, from a study by McMullin and Mundy (1992). This rich variety of molecular distributions is typical for such regions of massive star formation.

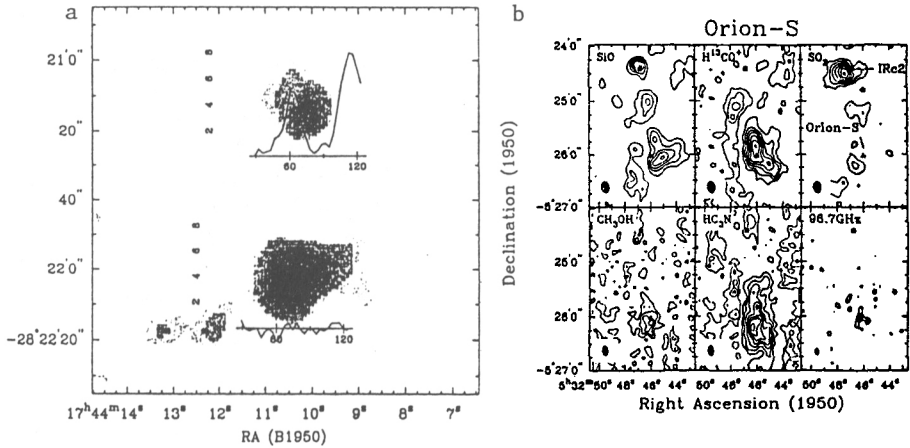


Figure 2. (a) SGR B2 in continuum (gray scale) and CH₃CH₂CN (line spectrum). (b) Multiple Molecular lines from a region 2 min south of Orion/KL.

Figure 3 shows results from observations of two sources within the solar system. On the left are the time series for flares detected toward an active region on the sun at 88 GHz (Kundu et al, 1989). The rapidly accelerated plasma that produces these high frequency radio flares is thought to also produce gamma rays as it propagates down magnetic field lines and strikes the denser solar atmosphere below. On the right is an image of the continuum emission from Mercury at 90 GHz (Mitchell and de Pater, 1992). The planet was at Elongation and Perihelion at the same time. The stronger thermal emission on the warmer sunlit side is clear. There is also an emission maximum on the opposite longitude which results from the greater average solar illumination there associated with the orbital/rotational resonance and the ellipticity of the orbit.

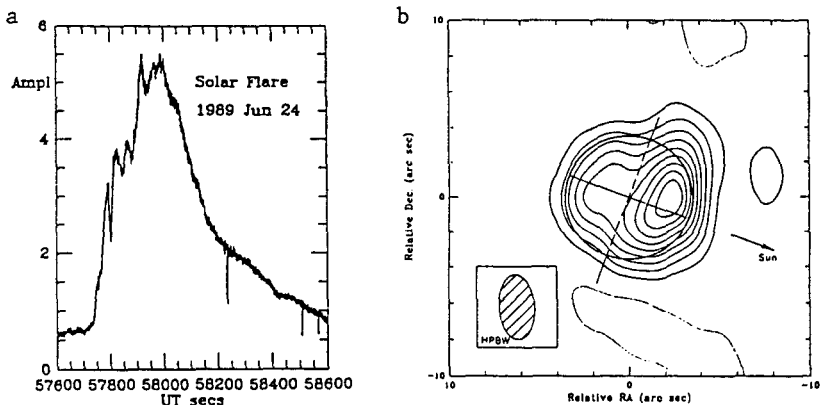


Figure 3. (a) 3mm solar flare. (b) continuum image of Mercury.

THE EXPANDED ARRAY

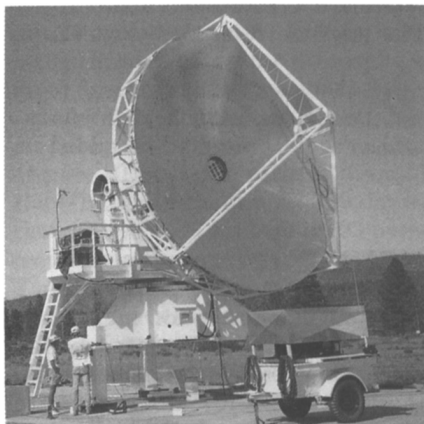
The array is currently being expanded from three to nine antennas. In addition the IF bandwidth has increased to 830 MHz, operation at 210 - 270 GHz with SIS receivers is being added, the spectral line correlator maximum bandwidth is now 800 MHz, the operating system is changed from VMS to UNIX, and an entirely new data reduction package, MIRIAD, has been developed (Crutcher, this volume). Table 1 summarizes the system properties, including the expected sensitivities.

| | | |
|----------------------------|-------------------------------|-------------------------------|
| Wavelength | 4.2mm - 2.6mm | 1.4mm - 1.1mm |
| Bands | 75 - 115 GHz | 210 - 270 GHz |
| Surfaces(20um RMS) | 1/150 wave | 1/50 wave |
| Primary Beam | 120 arcsec | 44 arcsec |
| Spectrometer(512 channels) | | |
| Max. BW (800 MHz) | 2400 km/sec | 880 km/sec |
| Best Resol. (10 kHz) | 0.3 km/sec | 0.1 km/sec |
| Receivers | SIS | SIS |
| T(DSB) | 50K | 100K(goal) |
| Best Resol. | 1.5 arcsec | 0.5 arcsec |
| Cont. Sens. (10h) | 0.4 mJy | 1.4 mJy |
| Line Sens. (10h) | | |
| (1 MHz Resolution) | del TB = 1.4K (1.5" pixel) | del TB = 2.4K (0.5" pixel) |

Table 1. Properties of the BIMA array of nine elements at both three and one millimeters wavelength.

The architecture of the correlator is described by Urry et al (1985). The new version is based on the NFRA correlator chip (Bos, 1987). The four window bandwidths may now be set to 200 MHz, 100 MHz, 50 MHz, 25 MHz, 12.5 MHz, or 6.25 MHz, with the use of time multiplexing to achieve the wider bandwidths. Each window may be set to any frequency in the 830 MHz IF band. Two different resolutions may be used simultaneously.

Figure 4A shows one of the new antennas, and 4B summarizes the reflector accuracies. The panel adjustment screws are operated from the front. The panels retain a light scallop from the machining which scatters sunlight when the sun is being observed but does not significantly affect the surface accuracy for millimeter wavelengths. The antennas employ roller drives with no backlash, and optical pointing is accurate to about 2". The receivers are located at the Cassagrain focus, where the focal ratio is F/4.8.

ANTENNA PROPERTIES

Diameter: 6m

Cass. f/D: 4.8

Drives: pinch-roller

Optical Pointing: 2" RMS (measured)

Expected Surface PrecisionPanels: 8 μ RMS (measured)Secondary: 5 μ RMS (measured)Gravity Deflection: 10 μ RMS (calculated)Holographic Setting: 10 μ RMS (measured)Total: $\leq 20\mu$

Figure 4. (a) One of the new BIMA antennas. (b) Reflector accuracies.

Figure 5 is a diagram of the dewar, which contains the receivers for all four of the bands that will be used. All of the receivers are slightly off axis, and the choice of observing band is made by simply changing the pointing of the antenna. The lens at the dewar window places the feed horn and its lens at the tertiary focus of the antenna. The expected (theoretical) aperture efficiency is about 84 percent.

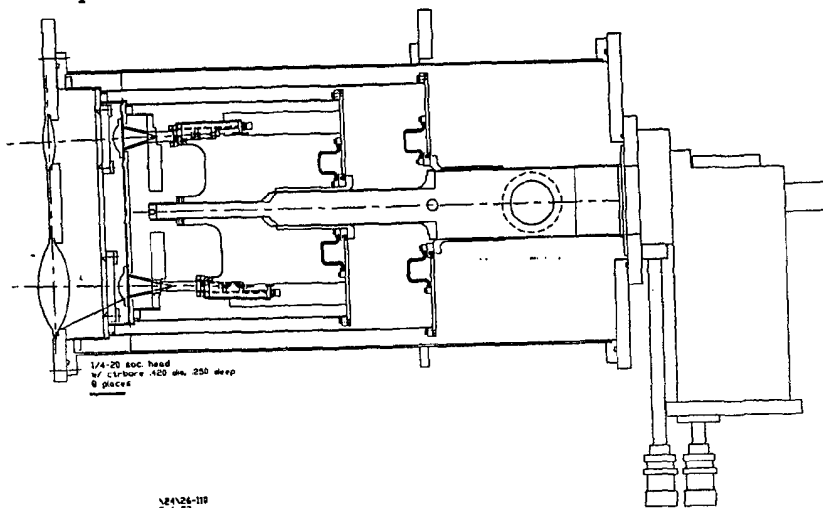


Figure 5. A diagram of the 12 inch diameter Dewar which has room for receivers for four bands.

The Figure also shows the three stage 4K refrigerator used to cool the SIS mixers. This refrigerator is a new development, a Gifford-McMahon type refrigerator, using a new regenerator material, Er₃Ni, developed at Toshiba, in

its third stage. Our machine consists of a standard CTI Model 1020 with a third stage added containing the ER3Ni. The machine cools to below 4K in about four hours with its 50mw load.

At the present writing, the first stage in the expansion, to six antennas, is nearly complete. The remaining three antennas are expected to be added in about one more year.

COMPENSATION FOR ATMOSPHERIC "SEEING"

The principal limitation to the formation of high angular resolution maps from interferometer arrays is the fluctuation in the visibility phase introduced by the atmosphere at widely separated antenna spacings. Whereas the atmospheric fluctuations that limit resolution at visible wavelengths to a few arc seconds are due to small scale density variations in the atmospheric oxygen and nitrogen, the corresponding fluctuations at radio wavelengths are caused by water vapor and have much larger scale sizes. The reason for the greater effect of the water vapor at the longer wavelengths is its permanent dipole moment and hence its much greater contribution to the index of refraction in this part of the spectrum.

If uncorrected, the radio wavelength phase fluctuations limit the achievable resolution to one or two arc seconds on the average, only a little better than optical "seeing". Recent measurements at the Plateau de Bure (Olimi and Downes, 1992), at Nobeyama (Kasuga et al, 1990), and at Mauna Kea (Masson, private communication) agree with the earlier observations of Armstrong and Sramek at the VLA (1982) which showed that the typical RMS phase fluctuations increase with antenna separation approximately as (*separation*)^{0.7}. This result indicates that better angular resolution is achieved at longer wavelengths. Thus, the situation steadily worsens as we extend operation into millimeter and sub-millimeter wavelengths. (Olimi and Downes, 1992) find a mean resolution limit of about two arc seconds at one millimeter for the Plateau de Bure. Phase correction by self-calibration has proven effective at the VLA and has enabled resolutions as high as .05" at one centimeter wavelength in the A array, for example. This technique requires many antennas and substantial source strengths to work, however, and will be less frequently useful at the shorter wavelengths where the sources are weaker.

We describe here preliminary results of experiments to test the idea of using measurements of fluctuations in the brightness of the atmosphere at millimeter wavelengths to correct for the phase fluctuations (Zivanovic, 1992). The premise is simple. Most of the emission from the atmosphere at millimeter wavelengths is due to water vapor along the line of site. Because the variable part of the phase is largely due to the same water vapor, the phase variations and the brightness variations should be well correlated, and it should be possible to use observations of the brightness changes to measure (and correct) the phase changes. Earlier experiments by Waters (1976) showed such a correlation, but probably because the beam of his water vapor radiometer was larger than the beam of his interferometer antennas and looked at a different part of the atmosphere, the strength of the correlation varied. The circumstances are more favorable at the shorter wavelengths where there is substantial atmospheric water vapor emission at all operating wavelengths, and one can detect the

brightness fluctuations as fluctuations in the receiver total power at any observing wavelength. In this case the interferometer observations are being made through the same atmosphere that is producing the corresponding water vapor brightness fluctuations.

Model calculations show that at 100 GHz a water vapor column that produces a brightness temperature of 1K produces a phase shift of about 200 degrees. This same ratio is about 100:1 at 250 GHz. To correct the phase at 100 GHz to an accuracy of 10 degrees, one must measure a receiver total power change of .05K. This is only .03 percent of a typical system temperature of 150K, requiring a receiver with a very stable gain and a wide continuum bandwidth. The important timescales for these fluctuations are 10-100 seconds, and the fractional receiver noise fluctuations are 2×10^{-5} for a 500 MHz bandwidth and 10 seconds integration time. This noise is no problem. The time interval between calibration of the visibility phase by observation of a calibration source, typically a quasar, is 15-30 minutes, and the gain must be stable over that interval. Stabilizing the detector gain to .01 percent may be accomplished by thermal regulation or perhaps by Dicke switching with a weakly coupled reference source at the input. Such stabilization is possible but requires care.

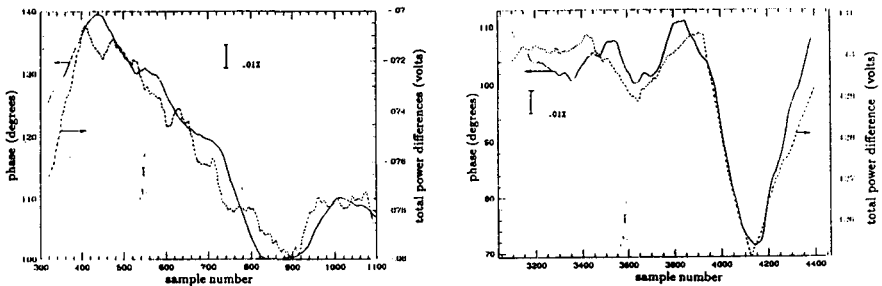


Figure 6. Two examples of the correlation between antenna total power difference and visibility phase.

Figure 6 shows two examples of the correlation of total power difference and visibility phase for a one baseline antenna pair at Hat Creek. Jupiter is the source, and the wavelength is 3.3 mm; the baseline length is 12 m. The time sample interval along the abscissa is 0.3 seconds, so that the figures show the correlation over intervals of 5-10 minutes. Also shown is a vertical bar corresponding to .01 percent of total power for each antenna. There is a clear correlation for the larger variations but a poorer correlation for the smaller scales. The smaller scale fluctuations may be dominated by gain variations. In any case, the phase fluctuations down to levels of 5-10 degrees are evidently being well measured, and correction to this level will produce very useful results.

As a simple test of the technique, we observed M87 in the continuum at 88 GHz with a single three baseline configuration, correcting the phase on each baseline according to the measured total power changes. Even though the map lacked much detail, being the result of a three baseline measurement, it was clearly improved by the phase corrections derived from the total power.

The map made using the corrections was substantially sharper than the map made without, which used only the observation of a calibrator at half hour intervals. Clearly, the scheme works at this level and shows promise of enabling interferometric mapping at longer baselines and higher resolution during times of typical atmospheric phase fluctuations. Note that this method has the advantage over self-calibration of providing the phase correction based on large scale brightness fluctuations of the atmosphere. Thus, it will work for sources of even very low flux. The principal technical challenge is the stabilization of the system gain to the .01 percent level over time intervals of 15 - 30 minutes. It clearly can be done, but it requires special care. It may be, for example, that for SIS mixers the gain stabilization must be done through Dicke switching with a weakly coupled input noise source. The experiments described here used a cooled Schottky mixer receiver which has intrinsically better gain stability.

ACKNOWLEDGEMENTS

It is a pleasure to thank a number of colleagues for providing me with results before publication. These include Lee Mundy, Joe McMullin, Lew Snyder, Xaolei Zhang, Mel Wright, Dick Plambeck, Naranjan Thatte, Dave Wilner, Lana Zivnovic, Jean Turner, Steve White, Mukul Kundu, Dave Mitchell, Imke de Pater, and John Lugten.

REFERENCES

- Armstrong, J. W., and Sramek, R. A. 1982, *Radio Sci.*, 17, 1579.
Bos, A. 1987, NFRA ITR no. 178.
Kasuga, T., Kanzawa, T., and Ishiguro, M. 1990, in "Radio Astronomical Seeing", eds. J. Baldwin and Wang Shoguan, Pergamon, Oxford, p. 54.
Kundu, M. R., White, S. M., Gopalswamy, N., and Bieging, J. C. 1989, *BAAS*, 21, 861.
McMullin, J., and Mundy, L. 1992, *Ap. J.*, in press.
Olmi, L., and Downes, D. 1992, *Astron. Astrophys.*, in press.
Snyder, L., Miao, Y., and Kuan, Y. J. 1992. *Ap. J.*, in press.
Waters, W. J. 1976, in "Methods in Experimental Physics", vol. 12B, ed. M. L. Meeks, Academic Press, NY, p. 142.
Wright, M. C., et al 1992, preprint.

DISCUSSION

Hall Given the poor site of the AT, we are particularly interested in the remote sensing of the water vapor to allow on-line phase correction. Our favored approach at the moment is to mount precision Water Vapor Radiometers on each telescope. We are looking at a precision digital back-end in the hope of achieving the required sensitivity. I would be interested in your comments on the relative merits of this approach and the 90 GHz differential continuum power measurements you referred to in your talk.

Welch If the separate water vapor radiometer is observing through a different column of atmosphere, there may not be a good correlation between the atmospheric brightness and the phase fluctuations. Measuring the atmospheric brightness changes by observing the received total power should insure a better correlation.

Ishiguro Two independent amplitude measurements are available in a two element interferometer. How do you incorporate these two independent amplitudes in your phase correction method?

Welch It is necessary to measure the difference between the total power outputs of the two antennas. Thus, you take the difference between the two amplitudes. The total power detectors must have gain stabilities of the order of 10^{-4} .

Ekers If you are testing the method of estimating atmospheric phase changes using total power changes on a strong source such as M87, you could make a more direct comparison with phases determined by self-calibration.

Welch That is an excellent suggestion. Thank you.